Separation Science and Technology
Publication details, including instructions for authors and subscription information:
http://www.informaworld.com/smpp/title~content=t713708471

A Comprehensive Study of Parameters Influencing the Performance of Multicomponent Adsorption in Fixed Beds

A. R. Mansour[a]; A. B. Shahalam[a]; Nayef Darwish[a]
[a] DEPARTMENTS OF CHEMICAL AND OF CIVIL ENGINEERING, YARMOUK UNIVERSITY, IRBID, JORDAN

To cite this Article Mansour, A. R. , Shahalam, A. B. and Darwish, Nayef(1984) 'A Comprehensive Study of Parameters Influencing the Performance of Multicomponent Adsorption in Fixed Beds', Separation Science and Technology, 19: 13, 1087 — 1111
To link to this Article: DOI: 10.1080/01496398408058350
URL: http://dx.doi.org/10.1080/01496398408058350

SEPARATION SCIENCE AND TECHNOLOGY, 19(13-15), pp. 1087-1111, 1984-85

A Comprehensive Study of Parameters Influencing the Performance of Multicomponent Adsorption in Fixed Beds

A. R. MANSOUR, A. B. SHAHALAM, and NAYEF DARWISH

DEPARTMENTS OF CHEMICAL AND OF CIVIL ENGINEERING
YARMOUK UNIVERSITY
IRBID, JORDAN

Abstract

A simplified mathematical model, developed earlier by Mansour, was used to carry out a comprehensive parametric study for the adsorption of a ternary system. This model was shown to satisfactorily match previously published experimental data. The effects of the following system parameters on the column performance are considered; height of the bed, initial concentration of solutes, fluid velocity, mass-transfer coefficients, size of particles, particle porosity, voidage of the bed, and the adsorption rate constants. The results presented here were compared with those of previous investigations and quite good agreement was obtained.

INTRODUCTION AND LITERATURE REVIEW

Adsorption onto activated carbon has found a wide acceptance as an effective process for purification of water and wastewaters. Since design of large-scale adsorbers is too expensive and since the theoretical concepts of multicomponent adsorption are lacking, an effective predictive model is required to facilitate simulation and parametric studies, and these should precede any design decision. The design of adsorption columns is closely related to the characteristic breakthrough curves. These are influenced to a large extent by the number of pollutants considered in the influent stream, and unlike the single solute case, multisolute adsorption is characterized by interactive and competitive effects involving various adsorbable species.

This article is concerned with investigation of the effects of most parameters affecting the design of multisolute adsorbers, using a fairly comprehensive model. A tri-solute system was used as a case study.

 0149-6395/84/1913-1087$3.50/0

However, the model used here has been shown (*13*) to be successfully used to work for any number of solutes without any modifications.

A survey of recent studies on adsorption indicates that most of these studies have dealt primarily with systems containing one adsorbable species, and the emphasis has been on developing mathematical models to simulate the actual process. No comprehensive studies have been performed on the effects of different parameters on the performance of multisolute adsorption columns. A fairly comprehensive review of previous studies is presented in Table 1.

GOVERNING EQUATIONS

For the isothermal, fixed-bed, multisolute adsorption problem considered in this study, it is assumed that an aqueous stream containing n adsorbable species of initially known concentration is flowed into a bed packed with spheres of activated carbon. It is assumed that the flow is uniform over the column cross-sectional area (that is, plug flow), and axial dispersion is negligible (*14*). Moreover, it was assumed that internal diffusion is a very rapid process. The governing equations for this model consist of two partial differential equations obtained from material balances on the fluid and solid phases. In addition, an equation describing the adsorption reaction rate is needed. For the general case, for any solute i, the governing equations can be written as

$$\frac{3}{R} K_{fi}(c_{di} - c_{pi}) - K_{1,i}(c_{si}^{*} - c_{si}) = \varepsilon_p \frac{\partial c_{pi}}{\partial t} \tag{1}$$

$$K_{1,i}(c_{si}^{*} - c_{si}) = \partial c_{si}/\partial t \tag{2}$$

A material balance applied to the adsorbate carried by the flowing fluid stream (the macro system) gives

$$\frac{\partial c_{di}}{\partial t} + \left[\frac{1 - \varepsilon_B}{\varepsilon_B}\right]\left[\frac{3K_{fi}}{R}\right](c_{di} - c_{pi})_{r=R} + \frac{V}{\varepsilon_B}\frac{\partial c_{di}}{\partial x} = 0 \tag{3}$$

The initial and boundary conditions needed to complete the description of the system are

$$\text{at } t = 0,\ C_{pi} \approx C_{si} = 0 \text{ for all } 0 \leq x \leq z$$

$$\text{at } t \leq 0,\ C_{di} \approx 0, \text{ for all } 0 \leq x \leq z$$

TABLE 1
Literature Review

Investigator	Gas or liquid	Number of components	Parameter									
			V (cm/s)	C_0 (g/cm^3)	Z (cm)	K_f (cm/s)	K_1 (s^{-1})	D_p (cm^2/s)	D_L	ε_p	ε_B	R (cm)
Balzli et al. (*1*)[b,c]	Liquid	2 and 3	Yes	Yes	Yes	No	No	No	No	No	No	No
Hsieh, Turian, and Tein (*7*)[a]	Liquid	2	No	No	No	Yes	No	No	No	No	No	No
Wilson (*21*)[a]	Liquid	1	Yes	Yes	No	No	Yes	Yes	Yes	Yes	No	No
Satter et al. (*17*)[a]	Liquid	1	Yes	Yes	No	No	No	No	Yes	No	No	No
Gariepy and Zwiebel (*6*)[a]	Gas	2	No	Yes	Yes	Yes	No	No	No	No	No	No
Liapis and Rippin (*10*)[b,c]	Liquid	2	No	No	No	Yes	No	Yes	No	No	No	No
Martin and Al-Bahrani (*15*)[c]	Liquid	1	Yes	Yes	Yes	No	No	No	No	No	No	Yes
Weber et al. (*19*)[b,c]	Liquid	1	Yes	No	No	No	No	No	No	Yes	No	No

[a]Numerical solution.
[b]Analytical solution.
[c]Experimental work.

$$\text{at } x = 0,\ C_{di} = C_{di_0}, \text{ for all } t$$

The following empirical equation, developed by Fritz and Schluender (*5*), was used to describe the multicomponent adsorption equilibria:

$$c_{si}^{*} = \frac{a_{i0} c_{pi}^{\ b_{i0}}}{ci + \sum_{j=1}^{n} a_{ij} c_{pj}^{\ b_{ij}}} = f_i(c_{p1}, c_{p2}, \ldots, c_{pn}) \tag{4}$$

The equilibrium isotherms determined for ternary system considered here have the following form (*1*):

$$c_{s1}^{*} = \frac{1.05 c_{p1}^{1.134}}{c_{p1}^{0.73} + 1.44 c_{p2}^{0.793} + 0.53 c_{p3}^{0.467}} \tag{5}$$

$$c_{s2}^{*} = \frac{1.09 c_{p2}^{1.182}}{c_{p2}^{0.831} + 0.52 c_{p1}^{0.884} + 0.30 c_{p3}^{0.536}} \tag{6}$$

$$c_{s3}^{*} = \frac{0.79 c_{p3}^{0.224}}{c_{p3}^{0.002} + 1.07 c_{p1}^{0.286} + 0.79 c_{p2}^{0.235}} \tag{7}$$

where butanol-2 is taken as Component 1, *t*-amyl alcohol as Component 2, and phenol as Component 3.

For many cases the concentration of the sorbate in the fluid phase does not change rapidly with time at a given point x. Thus, the time derivative, $\partial C_d / \partial t$ is much smaller than the spatial derivative $(V/\varepsilon_B)(\partial C_d / \partial x)$ and so can be neglected in Eq. (3). Therefore, after the solution of this model had been started, an abbreviated equation (after dropping the term $\partial C_d / \partial t$) could be used (in a further study) to reduce the computation time considerably.

METHOD OF SOLUTION

For any solute i, Eqs. (1) and (2) are coupled in the highly nonlinear C_{si}^{*} which is given in Eq. (4) and is expressed as $C_{si}^{*} = C_{pi}F(C_{pA1}, C_{pA2}, \ldots, C_{pAn})$, where C_{pA}'s are the values of C_p's obtained from a previous iterations. Hence, substituting for C_{si}^{*} into Eqs. (1) and (2), and using the restriction $\Delta x/\Delta t = V/\varepsilon_B$ to minimize the truncation error (*18*) applying backward-finite differencing to Eqs. (1) and (2), and central differencing to Eq. (3), a set of three simultaneous finite difference equations (a complete description is given in detail in Ref. *13*) results, and these are iteratively solved for C_p's,

C_s's, and C_d's, and the solution has been shown to satisfactorily agree with experimental results. This solution has been recently published (*14*).

Based on the reliable numerical computations obtained from the model described, parametric analyses for nine important parameters were performed.

RESULTS AND DISCUSSION

Parametric Analysis

The purpose of this analysis is to study the effects of different parameters on the performance of fixed-bed adsorbers. Consider the base case with the parameters given in Table 2 (*1*). Computer runs were made by varying each parameter individually while holding the others constant at their average values. The range of values for each parameter encountered in practice and used by various investigators is shown in Table 3. The values used for different parameters are given in Table 4.

TABLE 2
Base Case Variables Values

Height of adsorber, z, cm	41.0
Radius of carbon particle, R, cm	0.05
Porosity of particles, ε_p, fraction	0.94
Voidage of bed, ε_P, fraction	0.45
Bulk velocity, V, cm/s	0.139
Initial concentration, C_{0i}, g/cm^3:	
Component 1, C_{01}	9.150×10^{-4}
Component 2, C_{02}	9.120×10^{-4}
Component 3, C_{03}	9.970×10^{-4}
Mass transfer coefficient K_{fi}, cm/s:	
Component 1, K_{f1}	2.120×10^{-3}
Component 2, K_{f2}	1.950×10^{-3}
Component 3, K_{f3}	2.170×10^{-3}
Adsorption rate constant, $K_{1,i}$, s^{-1}:	
Component 1, $K_{1,1}$	5.333×10^{-4}
Component 2, $K_{1,2}$	4.917×10^{-4}
Component 3, $K_{1,3}$	3.278×10^{-4}

TABLE 3
Parameters in Literature

Investigator	K_1 (s^{-1})	K_f (cm/s)	V (cm/s)	D_p (cm^2/s)	ε_p	ε_B	C_0 (g/cm)	Z (cm)	R (cm)
Klaus et al. (8)[a]	0.0712	—	0.22	9×10^{-6}	0.79	0.5	6×10^{-5}	101	0.062
Wilde[a]	—	—	0.272	7×10^{-6}	0.60	0.4	10^{-5}–10^{-4}	200	0.05
Hsieh et al. (7)[a,b]	$1.56–41.7 \times 10^{-4}$	—	0.272	—	—	—	$1–6 \times 10^{-6}$	76.2	—
Chakravorti and Weber (2)[a,b]	—	$0.711–1.1 \times 10^{-3}$	1.09–8.08	$2.5–8.3 \times 10^{-6}$	—	—	$2.4–5.4 \times 10^{-6}$	183	0.069–0.1248
Crittenden and Weber (3)[a,b]	—	2.35×10^{-3}	0.736–1.54	9.64×10^{-6}	0.85	0.45–0.43	$6.5–5.3 \times 10^{-6}$	30.5–88.6	0.0155–0.0765
Balzli et al. (1)[b]	$3.28–5.3 \times 10^{-4}$	$1.68–2.11 \times 10^{-3}$	0.14	$7.4–13 \times 10^{-6}$	0.94	0.45	$1–2 \times 10^{-3}$	41–287	0.05
Martin and Al-Bahrani (15)[b]	—	—	0.144	—	—	—	$0.125–5.3 \times 10^{-5}$	8–22.5	0.045–0.055
Range of variation	10^{-4}–10^{-1}	1×10^{-3}	0.2	10^{-6}–10^{-5}	0.8	0.45	10^{-5}	100	0.05–0.125

[a]Numerical work.
[b]Experimental work.

TABLE 4
Values of Parameters

Parameter	Values used
Z, cm	65, 100, 150, 200
ε_B, fraction	0.4, 0.6, 0.95
ε_p, fraction	0.6, 0.8, 0.96
R, cm	0.01, 0.1, 0.14
V, cm/s	0.1, 0.3, 0.5[a]
K_{f1}/K_{f2}, dimensionless	0.5, 1, 2
K_{f1}/K_{f3}, dimensionless	0.5, 1, 2
K_{f2}/K_{f3}, dimensionless	0.5, 1, 2
c_{01}, g/cm^3	4.575×10^{-4}, 9.15×10^{-4}, 1.83×10^{-3}
c_{02}, g/cm^3	4.56×10^{-4}, 9.12×10^{-4}, 1.824×10^{-3}
c_{03}, g/cm^3	4.985×10^{-4}, 9.97×10^{-4}, 1.994×10^{-3}
$K_{1,1}$, s^{-1}	2.6665×10^{-4}, 5.333×10^{-4}, 1.0666×10^{-3}
$K_{1,2}$, s^{-1}	2.4585×10^{-4}, 4.917×10^{-4}, 9.834×10^{-4}
$K_{1,3}$, s^{-1}	1.639×10^{-4}, 3.278×10^{-4}, 6.556×10^{-4}

[a]The base value of z is 100 cm.

Effect of Bed Depth on Breakthrough Curves

In column systems, carbon-bed depth affects the process performance through its effects on contact time, t_c ($t_c = Z/V$). Therefore, in selecting an appropriate carbon-bed depth, it is essential to consider the ranges of velocity to be used; as a general rule, the longer the contact time (i.e., increase in bed depth and/or decrease in flow rate), the higher the percentage of the ultimate capacity of carbon that can be realized before an appreciable breakthrough of influent organics occurs and carbon replacement becomes available.

For all carbon-bed depths considered in this study, the general patterns of the breakthrough curves were as expected; after the first trace of any solute in the effluent was observed, the effluent concentration rose first gradually and then sharply before reaching the value of the influent concentration, thus denoting exhaustion of the bed. This behavior was also experimentally observed by Martin and Al-Bahrani (*15*).

Figure 1 shows that breakthrough time, particularly that of the key component (key component is defined as that which has the largest affinity to be adsorbed), which is Component 3 (i.e., phenol), is affected to a large extent by variation of bed depth; earlier breakthrough is obtained for

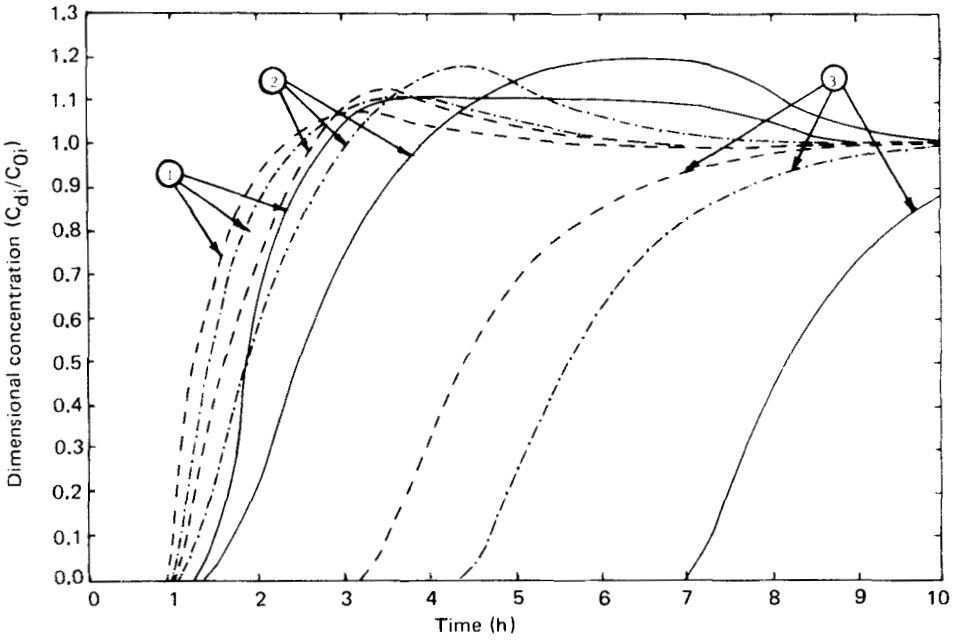

FIG. 1. Effect of bed height (z) on predicted breakthrough curves. z values: ——, 200; - · , 150; - -, 100.

shorter columns. This is a direct result of the low contact time for shorter depths. Moreover, Fig. 1 indicates that there is a strong relationship between the peak height of one nonkey solute and the height of the bed; the longer the bed, the larger the total amounts of the nonkey components (Solutes 1 and 2) displaced; hence the peak will increase as the depth of the bed increases. Moreover, the separation among the fronts increases in longer beds as shown in Fig. 1. Hence, for a given isotherm, there is a critical bed length beyond which the extra amounts of the nonkey components displaced can no longer catch up with front and add to the peak height. Figure 1 also shows another observation; the overshoot time interval increases with an increase in bed height; this is a result of the fact that for longer beds, larger amounts of the nonkey components are adsorbed and hence need a larger time interval to be displaced. These observations are in agreement with those of Balzli et al. (*1*), Martin and Al-Bahrani (*15*), and Gariepy and Zwiebel (*6*).

For single-solute systems, it was found (*15*) that the breakpoint (defined as the time corresponding to $C_d/C_0 = 0.1$) varies linearly with the depth of the carbon bed for a given flow rate. This finding was also observed here for

the case of the ternary system considered in this study as Fig. 2 shows. Since the breakpoint is considered to be the point at which effluent concentration exceeds the desirable limit, then the direct proportionality between the bed depth and the breakpoint has a significant practical importance; that is, the critical bed depth corresponding to zero breakpoint time may be determined. In this study the critical bed depth was, as Fig. 2 indicates, about 8 cm.

Effect of Initial Concentration on Breakthrough Curves

Feed composition is one of the most important parameters affecting the design of continuous adsorption columns. This is because, in actual adsorption processes, we expect to deal with feeds of different compositions, ranging from the very dilute solution mixtures to those which are highly concentrated (enriched mixtures). It then becomes necessary to investigate the influence of varying inlet concentration of different solutes on breakthrough curves.

For single—and binary—solute systems it has been found by many researchers (*6, 15, 21*) that, regardless of the component considered, the

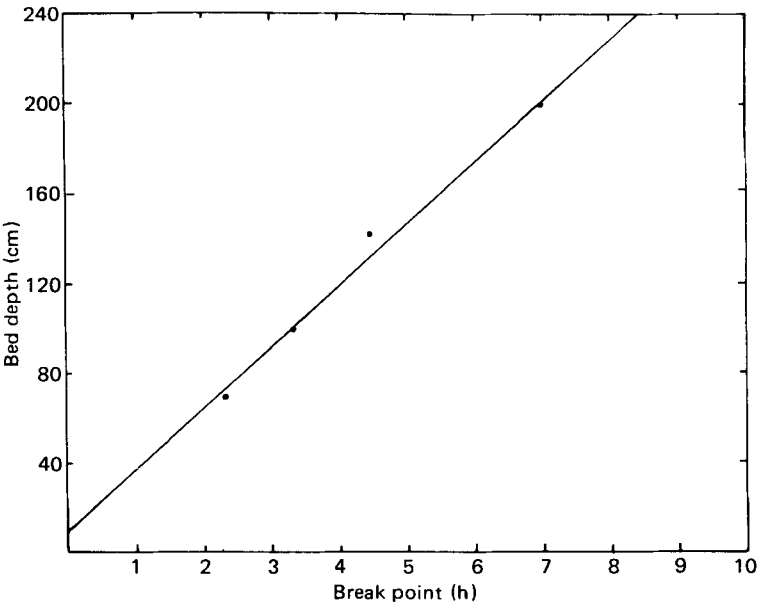

FIG. 2. Effect of carbon bed depth on break point time.

breakthrough curves sharpen whenever inlet concentrations are increased. This behavior was also observed for the simultaneous adsorption of the ternary system considered in this study.

When the inlet composition of the nonkey components (Components 1 and 2) was varied, an inverse variation of the peak composition (reached by the same nonkey components) was observed. No significant effect was observed in the breakthrough of the key component (Component 3) as shown in Figs. 3 and 4. This is a result of the relative competition on the adsorbent surface among different sorbates; the extent of adsorption (adsorbability) of each component is a function of the relative pure component affinity as well as the relative concentration (*6*). Hence, with the affinities specified for the system considered, the nonkey component adsorbability is decreased with decreasing composition, which means that it is more readily displaced downstream. Consequently, higher peaks were obtained when a more dilute mixture was used. On the other hand, the key components showed no response because their affinities are much larger than those of nonkey components and hence the effects of relative affinity

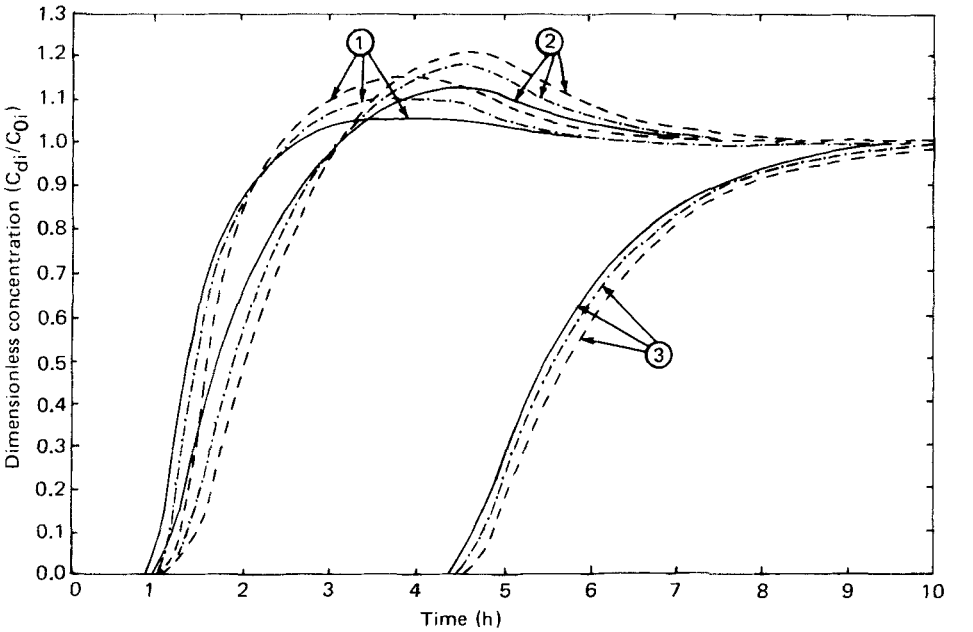

FIG. 3. Effect of initial concentration (C_{01}) of nonkey Component 1 (butanol-2) on predicted breakthrough curves. C_{01} values (in g/cm^3): ——, 1.83×10^{-3}; - -, 9.15×10^{-4}; - -, 4.575×10^{-4}.

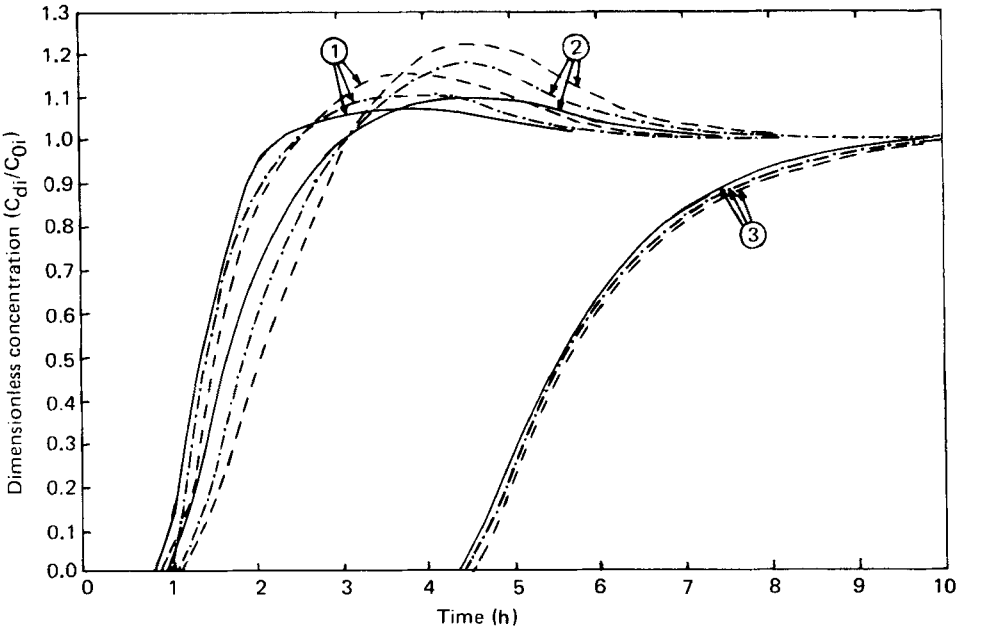

FIG. 4. Effect of initial concentration (C_{02}) of nonkey Component 2 (*t*-amyl alcohol) on predicted breakthrough curves. C_{02} values (in g/cm^3): ——, 1.82×10^{-3}; - -, 9.12×10^{-4}; - - 4.56×10^{-4}.

predominate while the relative concentration becomes less significant, which means that adsorbability (or breakthrough curves) of the key component is determined by its relative affinity which differs from one mixture to another. However, this phenomenon is not in accord with the studies (*6*) on a bi-solute gas mixture where it was reported that the breakthrough curves of the key component were affected to a large extent by the variation of the inlet concentration of the nonkey components.

On the other hand, when the inlet concentration of the key component was varied, pronounced effects were observed in the breakthrough curves of both the key and the nonkey components; a decrease in the inlet concentration of the key component from 19.94×10^{-4} to 4.983×10^{-4} g/cm^3 is shown to delay the breakthrough of the key component itself by about 5.2 h as Fig. 5 indicates. This is physically expected, since the adsorbent bed has a specified utilization capacity.

To summarize, the nonkey components respond toward the initial concentration of the key component in three ways: (1) the overshoot time interval decreases with an increase in the inlet concentration of the key

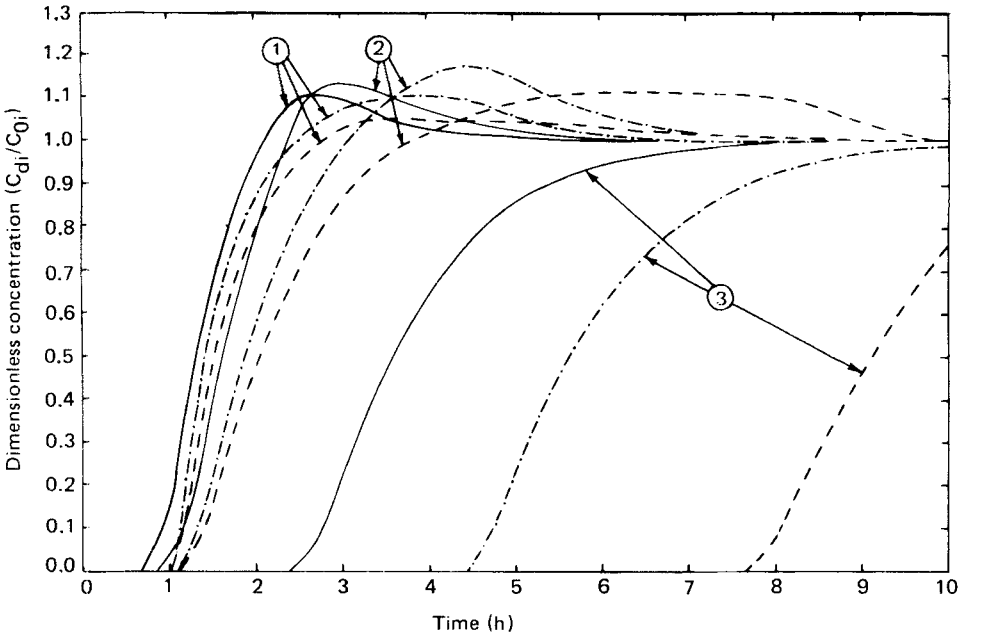

FIG. 5. Effect of initial concentration (C_{03}) of key Component 3 (phenol) on predicted breakthrough curves. C_{03} values (in g/cm^3): ——, 1.994×10^{-3}; - -, 9.97×10^{-4}; - -, 4.985×10^{-4}.

component, and this is a result of the fact that higher concentrations of the key component displace a specified amount of adsorbed nonkey solutes in shorter time intervals; (2) the peaks of the nonkey component profiles increase with increasing inlet concentration of the key component, and this is because, at higher concentrations, the key component has a greater competitive edge, and consequently more of the nonkey solutes are displaced; (3) the breakthrough time of the nonkey components is affected, but slightly, by the increase in the key-component inlet concentration (an increase from 4.983×10^{-4} to 19.94×10^{-4} caused an earlier breakthrough of the nonkey components by a maximum time of 25 min only, as Fig. 5 shows).

Effects of Bulk Velocity on Breakthrough Curves

Physically, bulk velocity V is expected to have effects on column behavior which are directly opposite to those of bed height Z, since both of

V and Z affect column performance through their effects on contact time t_c ($t_c = Z/V$). Many investigators (*15, 17*) have shown that for a single-component system, as a general rule, sharper breakthrough curves result from an increase of flow rates. This effect seems to be the case for multicomponent (ternary) systems, as Fig. 6 reveals. This can be partly attributed to a larger amount of solute coming into contact with the carbon per unit time, which results in a faster approach to breakpoint and exhaustion capacity. Furthermore, a higher flow rate means a shorter contact time between the carbon and the solute, and therefore allows more chance for the solute to escape into the effluent stream. Now it can be easily understood why the key component does not emerge in the effluent during the first 10 h of operation for the small velocity of 0.1 cm/s, as shown in Fig. 6. It is worth noting here that an increase of the volumetric flow rate through the column results in some deterioration of column performance, as illustrated in Fig. 6.

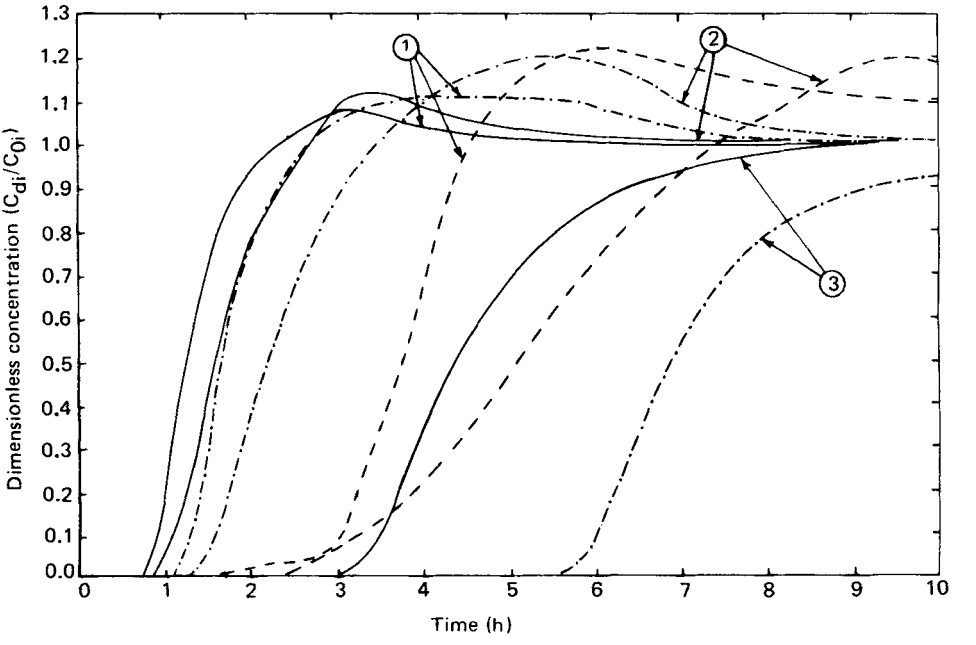

FIG. 6. Effect of bulk velocity (V) on predicted breakthrough curves. V values (in cm/s): ——, 0.5; - ·, 0.3; - -, 0.1.

Effect of Particle Size on Breakthrough Curves

For different particle sizes in a single component system, it was shown (*14, 15*) that a strong influence occurs at early breakthrough times; the bed of smaller particles produced higher initial removal of the solute but sharper breakthrough curves.

The effect of particle size in a ternary adsorption system is shown in Fig. 7. The effect on the key component behavior is seen to be pronounced and resembles that of a single component adsorption system, whereas the nonkey components show no signficant effects on their breakthrough curves. The effect of particle size on the column performance can be expressed in terms of two factors. The first is the mass transfer coefficient and the outside surface per unit volume. When particles are first contracted by liquid-containing sorbates, the rate of mass transfer is controlled by the outside film resistance (low velocity is assumed); however, the effect of this factor is the same in all three cases shown in Fig. 7. Since all of them have

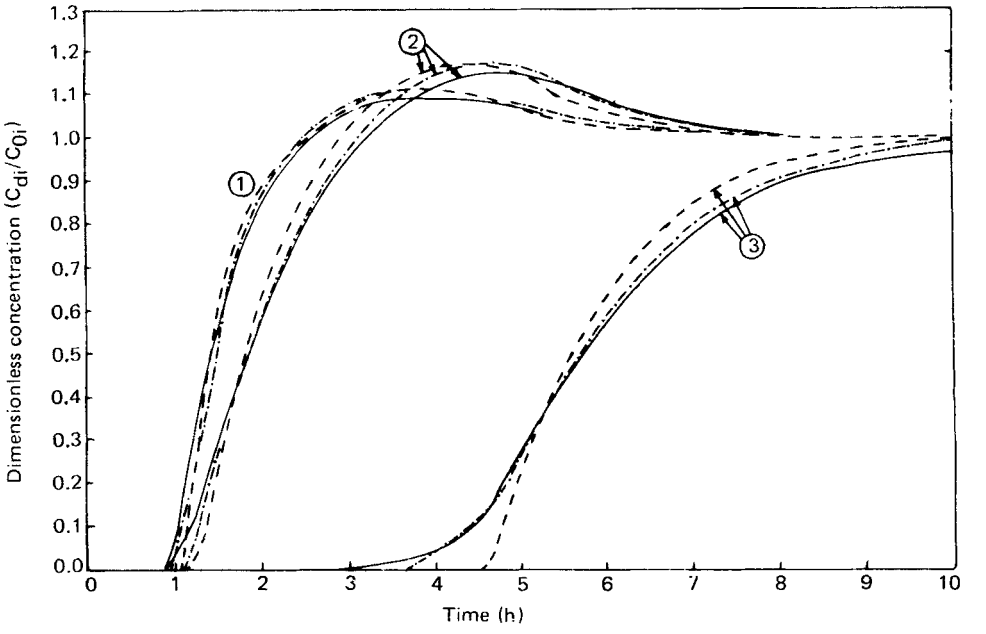

FIG. 7. Effect of particle size (average radius R) on predicted breakthrough curves. R values (in cm): ——, 0.14; - -, 0.1; - -, 0.01.

the same inlet concentration, the rate of mass transfer is proportional to the product of the mass transfer coefficient and the outside area of the particles per unit volume of the bed. Since this product for the 0.14-cm particles is the smallest, the mass transfer rate of solute is initially slower. The second factor that causes breakthrough to be the earliest for the system of largest particles is that for a given particle, as time proceeds and the external surface area becomes essentially saturated with adsorbate, the pore diffusional resistance becomes increasingly significant, and since the largest particles have the longest diffusional paths, they would be expected to have the earliest breakthrough. Figure 7 shows that the breakthrough curves for each component intersect, and this is expected since the area above the curves is related to ultimate holdup of beds which have the same mass of particles and the particles are assumed to have essentially the same capacities. Furthermore, we can see that smaller spheres contribute less to peak spreading, as expected. Nevertheless, the effect of particle size is much less than those of parameters related to mass transfer processes.

Another observation to be reported for the first time: The effect of the variation of carbon particle size described above increases as the adsorbability of the solute increases. Therefore, as Fig. 7 indicates, the strongest sorbate (most adsorbable), i.e., phenol, shows the largest effect by variation of particle radius.

To summarize: During the first hours of operation, the column adsorption process is controlled by the external film resistance, and when the external surface of the particles becomes saturated, the process is controlled by pore diffusion.

Effect of Porosity of the Particles on Breakthrough Curves

Figure 8 shows that three different values of the porosity of particles produce almost the same breakthrough curves for the three components considered in this study. This is mathematically expected, since we assume both pore and surface concentrations to be independent of the particle radius (i.e., $C_p \neq C_p(r)$ and $C_s \neq C_s(r)$). However, the porosity of the particle, ε_p, is still present in the governing equation, Eq. (1), i.e., $\varepsilon_p(\partial C_p/\partial t)$, but is known from practice that the term $\partial C_p/\partial t$ is very small since the accumulation of sorbates in the liquid phase in a particle is negligible. Hence, the porosity of particles has no noticeable effect on breakthrough curves when a simplified model is used; however, this may not be the case for nondilute systems.

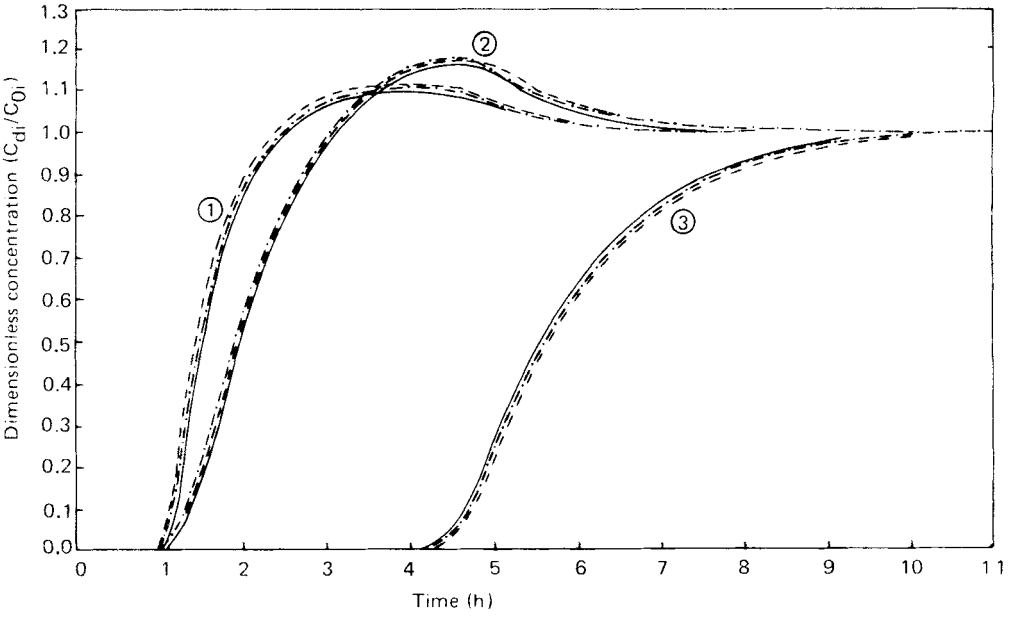

FIG. 8. Effect of particle porosity (ε_p) on predicted breakthrough curves. ε_p values: ——, 0.96; - -, 0.8; - -, 0.6.

Effect of Bed Voidage on Breakthrough Curves

Figure 9 shows that bed voidage affects the column performance to a large extent; sharper and earlier breakthrough curves and lower peak heights result from an increase of bed voidage. The key component as well as the nonkey components are seen to be highly affected. The breakthrough time for the key component (time corresponding to breakpoint) is seen to be reduced from 5 to 0.7 h by increasing the bed voidage from 0.4 to 0.95,* an effect which is pronounced. This can be attributed to the fact that the bulk velocity (which is equal to the free stream velocity multiplied by the bed voidage) is higher for higher bed porosity, hence a smaller contact time for larger porosity allows more chance for the solute to escape into the effluent stream. Therefore, the breakthrough time for the key component, as seen in Fig. 9, approaches those of nonkey components, and this is evident for the highest bed voidage of 0.95 where the breakthrough time for the three

*It is obvious that $\varepsilon_B = 0.95$ is not a practical value. It was used for investigation purposes only.

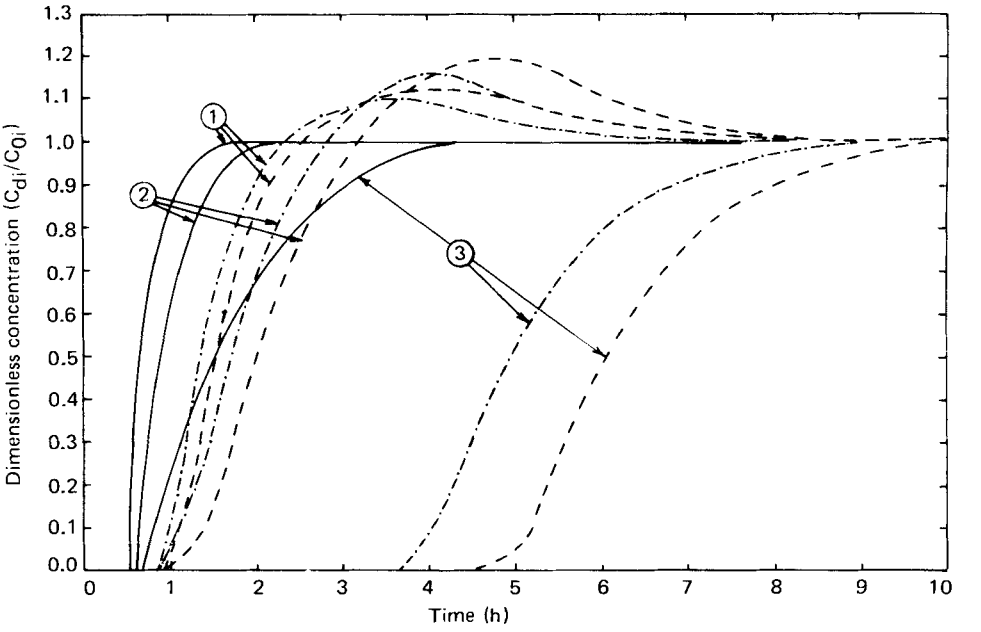

FIG. 9. Effect of bed voidage (ε_B) on predicted breakthrough curves. ε_B values: ——, 0.95; · ·, 0.6; - -, 0.4.

components is nearly the same. It is worth noting that no overshoot (peak height is equal to zero) is observed for a bed porosity of 0.95, which is physically expected, since at high bed voidage the so-called channeling becomes most probable.

Effects of Adsorption Rate Constants on Breakthrough Curves

Effects of adsorption rate constants on the breakthrough curves of the simultaneous adsorption of the ternary system are illustrated in Figs. 10, 11, and 12. Increasing the adsorption rate constant of the nonkey components ($K_{1,1}$ and $K_{1,2}$) is seen in Figs. 10 and 11 to affect only the breakthrough curves of the same nonkey components. The peak heights increase with increasing adsorption rate constants. This is expected for higher values of $K_{1,1}$ and $K_{1,2}$ since larger amounts of the nonkey components are adsorbed. It can also be seen (Figs. 10 and 11) that the adsorption rate constants of the nonkey components affect the breakthrough time of the same nonkey components, but to a smaller extent.

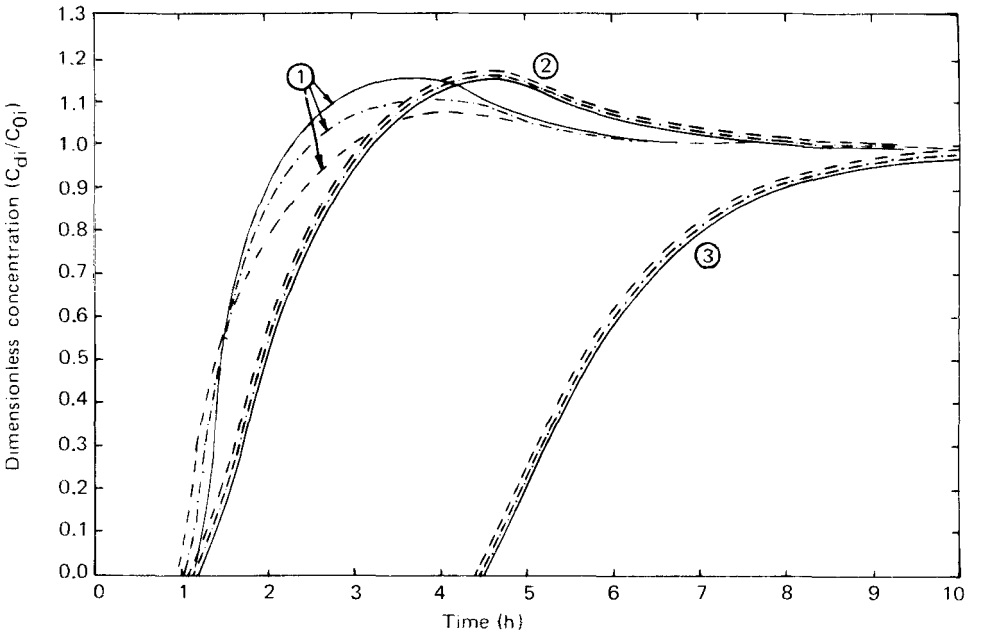

FIG. 10. Effect of adsorption rate constant ($K_{1,1}$) of nonkey Component 1 (butanol-2) on predicted breakthrough curves. $K_{1,1}$ values (in s^{-1}): ——, 1.0666×10^{-3}; - -, 5.333×10^{-4}; --, 2.665×10^{-4}.

Hence, varying the adsorption rate constants of nonkey components has almost no effect, at least for dilute systems, on other components (the key ones) in a multicomponent adsorption system. On the other hand, Fig. 12 shows that varying the adsorption rate constant of the key component ($K_{1,3}$) affects the breakthrough curves of both the key and the nonkey components, but the effects are profound for the key component. It can be seen from Fig. 12 that increasing $K_{1,1}$ results in a very marked improvement in the shape of the breakthrough curves of the key component. Leakage through the column before saturation is drastically reduced. This is a result of the fact that increasing the adsorption rate constant reduces the external film resistance and hence equilibrium between solid and liquid phases becomes probable. It is worth noting that the three breakthrough curves for the key components cross each other at the same point (Fig. 12). This is because the area above each of them is related to the total adsorption capacity which is fixed for the same system.

Figure 12 also shows that the breakthrough curves of Component 2 (*t*-amyl alcohol) is affected by varying $K_{1,3}$; the peak height increases with

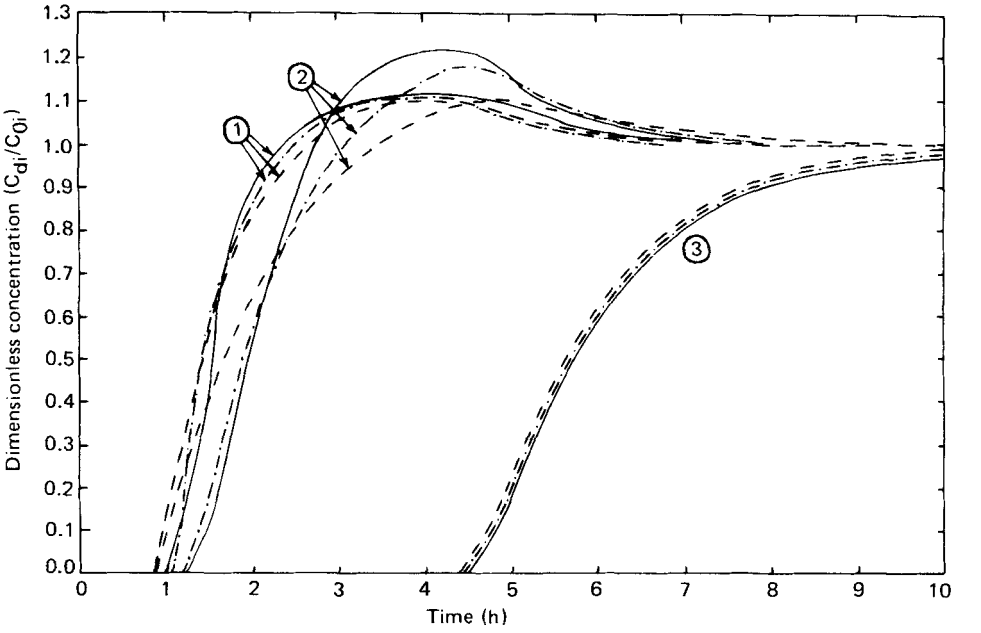

FIG. 11. Effect of adsorption rate constant ($K_{1,2}$) of nonkey Component 2 (*t*-amyl alcohol) on predicted breakthrough curves. $K_{1,2}$ values (in s^{-1}): ——, 9.834×10^{-4}; - -, 4.917×10^{-4}; - - 2.4585×10^{-4}.

increasing $K_{1,1}$ whereas the effect on the breakthrough curves of Component 1 (butanol-2) is negligible. This may be attributed to the individual chemical properties of Components 1 and 2.

One more important observation should be made: Since the system considered in this study is dilute, we expect that mutual interactions will be negligible.

Effects of Mass-Transfer Coefficients on Breakthrough Curves

The concentration profile of an adsorbed material in a column is determined by the interaction between the fluid–solid equilibrium and the mass transfer process taking place. The concentration profile for the adsorption of a single component in a liquid system was found to be strongly affected by the external film resistance (*1*); the concentration change becomes less abrupt as the film resistance increases. A very strong influence due to external film resistance was also observed for the

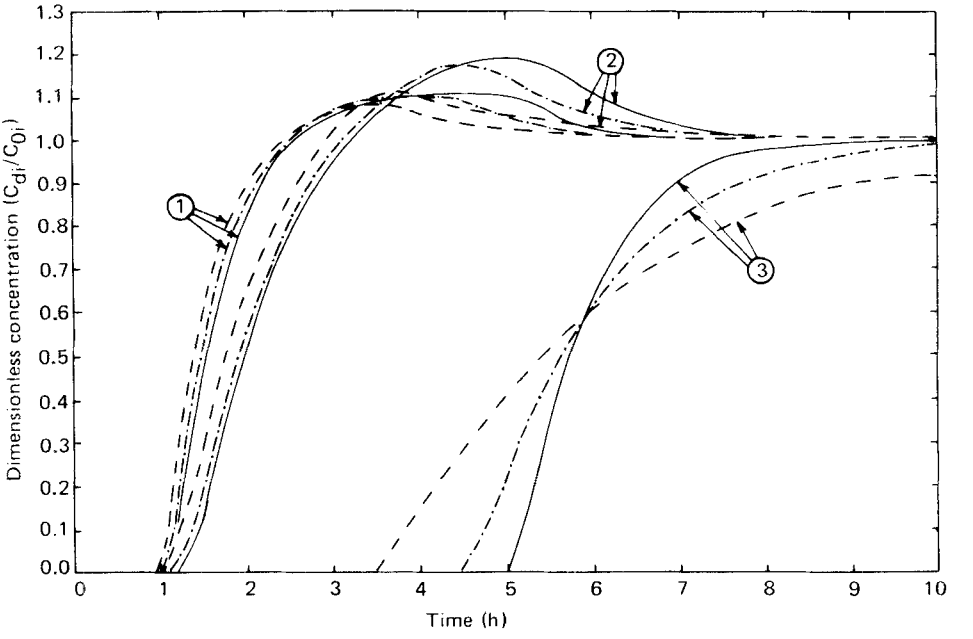

FIG. 12. Effect of adsorption rate constant ($K_{1,3}$) of key Component 3 (phenol) on predicted breakthrough curves. $K_{1,3}$ values (in s^{-1}): ——, 6.556×10^{-4}; - -, 3.278×10^{-4}; - -, 1.639×10^{-4}.

adsorption of a binary gaseous mixture (*6*). The relative mass transfer rates exert a pronounced influence on the breakthrough curves, so much that the order of appearance of the components may be reversed.

Liquid-to-particle mass transport effects are usually small in commercial columns. Hence, as shown in Figs. 13 and 14, breakthrough curves of the less adsorbable species (nonkey components) are not affected by variation of their mass-transfer coefficients. On contrast, the breakthrough curves of the strongest adsorbable solute (key component) are greatly influenced by variation of the ratio K_{f2}/K_{f3} as Fig. 15 shows.

CONCLUSIONS

The parametric studies for the adsorption of a ternary system (butanol-2, *t*-amyl alcohol, and phenol) in a fixed bed have been found to affect the adsorption column performance as follows:

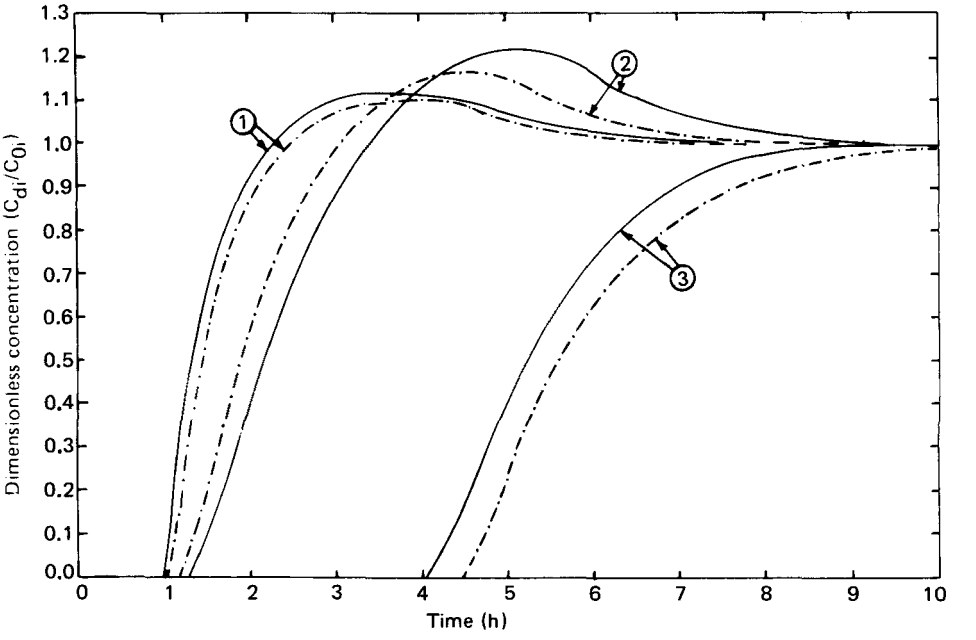

FIG. 13. Effect of mass transfer coefficients ratio (K_{f1}/K_{f2}) on predicted breakthrough curves. K_{f1}/K_{f2} values: ——, 2; - · -, 1; - -, 0.5.

1. Peak heights of the nonkey components (butanol-2, *t*-amyl alcohol) breakthrough curves increase with bed length up to a critical length. Thereafter they remain constant with a general broadening of the peaks.
2. Varying the inlet compositions of the two nonkey components will have the most significant effects on the peak heights of the nonkey component breakthrough curves. Peak heights increase with decreasing nonkey components' concentrations at a constant composition of the key component.
3. Varying the key component inlet concentration will affect the breakthrough curves of both the key component and the nonkey components. The sharpness of the key components' breakthrough curves are inversely affected (the lower the concentration the broader the curve), whereas peak heights of the nonkey components decrease with decreasing concentration of the key component at fixed concentrations of nonkey components.

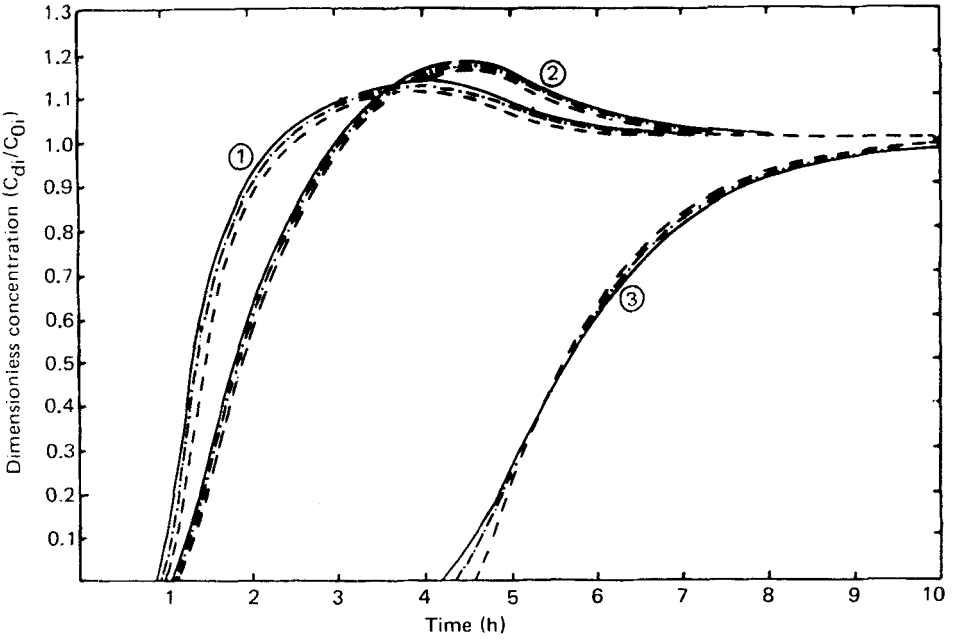

FIG. 14. Effect of mass transfer coefficients ratio (K_{f2}/K_{f3}) on predicted breakthrough curves. K_{f2}/K_{f3} values: ——, 2; - ·, 1; - -, 0.5.

4. Sharper breakthrough curves of the key and the nonkey components result from an increase of bulk velocity.
5. During the first hours of operation, the column adsorption process is controlled by the external film resistance, and when the outer surface of the particles becomes saturated, the process is controlled by the pore diffusion.
6. The porosity of the particles has no effect when simplified model for dilute solutions is used.
7. Sharper and earlier breakthrough curves and lower peak heights result from increasing the bed voidage. Higher values of bed voidage lead to so-called channeling.
8. Varying the adsorption rate constants of the nonkey components affects only the breakthrough curves of the same nonkey components. The peak heights increase with increasing adsorption rate constants. Increasing the adsorption rate constant of the key component results in a very marked improvement in the shape of the breakthrough curves of the key component.

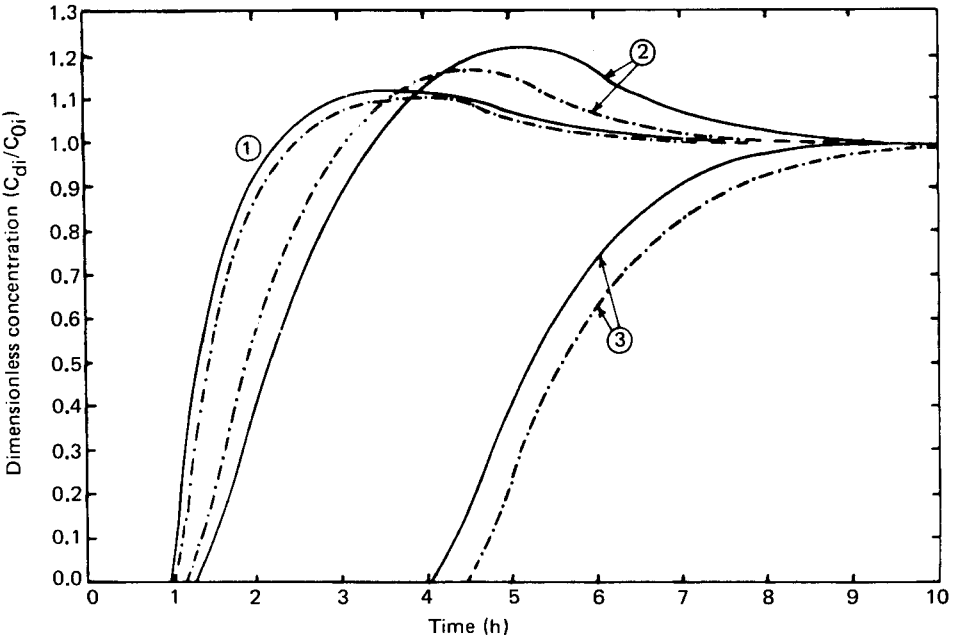

FIG. 15. Effect of mass transfer coefficients ratio (K_{f2}/K_{f3}) on predicted breakthrough curves. K_{f2}/K_{f3} values: ——, 5; ··, 1.

9. For dilute mixtures, mutual effects for different solutes can be neglected.

SYMBOLS

a_{i0}, a_{ij}	coefficients in Eq. (4)
b_{i0}, b_{ij}	exponents in Eq. (4)
C_d	concentration of solute in fluid phase of the bed (g/cc)
C_0	the value of C_d at the entrance of bed
C_p	concentration of solute in pore fluid phase (g/cc)
C_s	concentration of solute in solid phase (per unit volume of particles) (g/cc)
K_f	mass transfer coefficient for liquid–particle transfer (cm/s)
K_1	adsorption rate coefficient (s^{-1})
R	average radius of particles (cm)
t	time (s)

t_c contact time (s)
V fluid velocity (cm/s)
X distance along bed (cm)
Z height of adsorber (cm)

Greek Symbols

ε_B bed void fraction
ε_p particle void fraction

Superscripts

* equilibrium value

Subscripts

i index for component number
p pore
s solid

Acknowledgment

The authors wish to thank the Computer Center at the University of Yarmouk for the services they afforded during our work on this project.

REFERENCES

1. Balzli, M. W., A. I. Liapis, and D. W. T. Rippin, "Applications of Mathematical Modelling to the Simulation of Multi-Component Adsorption in Activated Carbon Columns," *Trans. Inst. Chem. Eng., 56*, 145 (1978).
2. Chakravorti, R. K., and T. W. Weber, "A Comprehensive Study of the Adsorption of Phenol in Packed Bed of Activated Carbon," *AIChE Symp. Ser., 71*(151), 392 (1975).
3. Crittenden, J. C., and W. J. Weber, "Model for Design of Multicomponent Adsorption Systems," *J. Environ. Eng. Div., ASCE, 104*(EE6), Proc. Paper 1175 (December 1978).
4. Ford, D. L., and F. S. Manning, "Treatment of Petroleum Refinery Wastewater," in *Carbon Adsorption Handbook* (P. N. Cheremisinoff and F. Ellerbusch, eds.), 1978, p. 687.
5. Fritz, W., and E. V. Schluender, "Simultaneous Adsorption Equilibria of Organic Solutes in Dilute Aqueous Solutions on Activated Carbon," *Chem. Eng. Sci., 29*, 1279 (1974).

6. Gariepy, J. W., and I. Zwiebel, "Adsorption of Binary Mistures in Fixed Beds," *AIChE Symp. Ser., 67*, 17 (1971).
7. Hsieh, J. S. C., R. M. Turian, and Chi Tien, "Multicomponent Liquid Phase Adsorption in Fixed Bed," *AIChE J., 23*, 263 (1977).
8. Klaus, R., R. C. Aiken, and D. W. T. Rippin, "Simulated Binary Isothermal Adsorption on Activated Carbon in Periodic Countercurrent Column Operation," *Ibid., 23*(4), 579 (1977).
9. Kostecki, J. A., F. S. Manning, and L. N. Canjar, "The Kinetics of Physical Adsorption of a Binary Liquid System in Fixed Beds," *Chem. Eng. Prog. Symp. Ser., 63*(74), 90 (1967).
10. Liapis, A. K., and D. W. T. Rippin, "The Simulation of Binary Adsorption in Continuous Countercurrent Operation and a Comparison with Other Operating Modes," *AIChE J., 25*(3), 455 (1979).
11. Liaw, C. H., J. S. P. Wang, R. A. Greenkorn, and K. C. Chao, "Kinetics of Fixed-Bed Adsorption: A New Solution," *Ibid., 25*(2), 376 (1979).
12. Mansour, A. R., "Numerical Solution of Multi-Component Adsorption from a Stirred Bath," MS Thesis, University of Tulsa, 1979.
13. Mansour, A. R., "Numerical Solution of Liquid Phase Multicomponent Adsorption in Fixed Beds," PhD Dissertation, The University of Tulsa, 1980.
14. Mansour, A. R., D. U. Von Rosenberg, and N. D. Sylvester, "Numerical Solution of Liquid Phase Multi-Component Adsorption in Fixed Beds," *AIChE J., 28*(5), 765 (1982).
15. Martin, R. J., and K. S. Al-Bahrani, "Adsorption Studies Using Gas–Liquid Chromatography—III. Experimental Factors Influencing Adsorption," *Water Res., 12*, 879 (1978).
16. Reis, J. F. G., E. N. Lightfoot, P. T. Noble, and A. S. Chiang, "Chromatography in a Bed of Spheres," *Sep. Sci. Technol., 14*(5), 367 (1979).
17. Satter, A., Y. M. Shum, W. T. Adams, and L. A. Davis, *Chemical Transport in Porous Media with Dispersion and Rate-Controlled Adsorption*, Society of Petroleum Engineers, 1980, p. 129.
18. Von Rosenberg, D. U., *Methods for the Numerical Solution of Partial Differential Equations*, G. L. Farrar and Associates, Tulsa, Oklahoma, 1977.
19. Weber, T. W., and R. K. Chakravorti, "Pore and Solid Diffusion Models for Fixed-Bed Adsorption," *AIChE J., 20*(2), 228 (1974).
20. Weber, W. J., *Physicochemical Process for Water Quality Control*, Wiley-Interscience, New York, 1972.
21. Wilson, D. J., "Theory of Adsorption by Activated Carbon. II. Continuous Flow Columns," *Sep. Sci. Technol., 14*(5), 415 (1979).

Received by editor May 30, 1984